Available online at www.sciencedirect.com
SCIENCE DIRECT®
Biochemical and Biophysical Research Communications 329 (2005) 64–70
BBRC
www.elsevier.com/locate/ybbrc

Changes in adsorption and permeability of mitoxantrone on plasma membrane of BCRP/MXR resistant cells

G. Breuzard[a], O. Piot[a], J.-F. Angiboust[a], M. Manfait[a], L. Candeil[b], M. Del Rio[b], J.-M. Millot[a,*]

[a] *Unité MéDIAN CNRS UMR 6142, IFR 53, UFR de pharmacie, 51 rue Cognacq-Jay, 51096 Reims Cedex, France*
[b] *Génomique Fonctionnelle et Pharmacologie des Tumeurs CNRS UMR 5160, CRLC Val d'Aurelle—Bâtiment Recherche, 35 rue de la Croix Verte, 34298 Montpellier Cedex 5, France*

Received 18 January 2005
Available online 2 February 2005

Abstract

A selective analysis of adsorbed mitoxantrone (MTX) was performed by surface-enhanced Raman scattering (SERS) at the range of cellular membrane. Disruption of the membrane fluidity was carried out to appraise changes in membrane adsorption of MTX and drug uptake in sensitive (HCT-116 S) and resistant BCRP/MXR (HCT-116 R) cells. Based on spectral MTX modifications, micro-SERS spectroscopy discriminated clearly drug adsorption phenomena on plasma membrane from drug in solution. A 3-fold higher SERS intensity of MTX for HCT-116 R was observed concluding to a higher drug adsorption on resistant membrane. The increase of membrane fluidity with benzyl alcohol (BA) or chloroform (CF) resulted in a 3-fold decrease of MTX adsorption on HCT-116 R, exclusively. BA and CF improved intracellular accumulation of MTX (e.g., 823 and 191 pmol MTX/10^6 HCT-116 R incubated with or without BA). At 4 °C, drug accumulation measurements showed a decrease of MTX permeability in resistant membrane (42 pmol MTX/10^6 cells), restored with fluidizers (e.g., 342 pmol MTX/10^6 cells with BA). Fluorescence confocal microscopy involved an exclusive MTX emission around the plasma membrane of resistant cells whereas fluidizers increased the intracellular uptake of MTX in both cell lines at the same time with less drug emission around the plasma membrane. Changes of the membrane structure of resistant cells should modify both drug adsorption and membrane permeation.

Keywords: Mitoxantrone; Plasma membrane; Higher adsorption; Resistance; SERS

Optimization of drug influx and limitation of its efflux across the membrane barrier are two most important targets to increase the efficacy of chemotherapeutic drugs [1]. Drug resistance remains one of the primary causes of suboptimal outcomes in cancer therapy [2]. The multi-drug resistance (MDR) was determined with an efflux protein overexpression as the breast cancer resistant protein (BCRP) and changes of lipid composition. The decrease of intracellular accumulation of cytotoxic drugs could be dependent on a slower drug uptake through the plasma membrane [3]. Two different mechanisms were proposed to account for the solute permeation across lipid membranes such as (i) the diffusion through transient pores or defects in the membranes and (ii) partitioning into the hydrophobic phase of the bilayer followed by diffusion to the opposite side of the membrane [4].

A transfer step over the plasma membrane of most anticancer drugs implicates adsorption, insertion, and flip-flop that can be distinguished as consecutive stages in the transbilayer movements [5–7]. Hydrophobic interactions, membrane fluidity, and drug lipophilicity are decisive for efficient intracellular uptake of anticancer drugs [8,9]. Anthracyclines and mitoxantrone (MTX)

* Corresponding author. Fax: +33 3 26 91 35 50.
E-mail address: jm.millot@univ-reims.fr (J.-M. Millot).

0006-291X/$ - see front matter © 2005 Published by Elsevier Inc.
doi:10.1016/j.bbrc.2005.01.098

are probably the best-studied examples in drug-membrane interactions [10–12]. Different agents fluidizing membrane (anesthetics, chloroform, neutral mild detergents, and certain MDR-type drugs) have been described to modulate the uptake of doxorubicin [7,13]. Regev et al. concluded the transbilayer movement of the drug was only correlated with membrane fluidity and indicated that the step limiting the movement rate was located in the membrane matrix. Thus, the relation between drug adsorption in a cellular resistance model [12] and the intracellular uptake still remains unclear.

We have previously reported the higher mitoxantrone adsorption on the plasma membrane of resistant cells compared to its sensitive strain by surface-enhanced Raman scattering (SERS) spectroscopy [12]. Indeed, this method revealed to be a selective analysis of drug adsorption on membrane due to both high sensitivity (10^{-10} M drug) and to the exclusive analysis of drug near a surface. SERS is based on the enhancement by several orders of magnitude (up to 10^9 [14]) of the Raman intensity of molecules in the vicinity of a roughened metallic surface. This study aims to bring details about parameters allowing a modulation of membrane permeation of sensitive (HCT-116 S) and resistant BCRP/MXR (HCT-116 R) cells with fluidizers benzyl alcohol and chloroform. In addition, a relation between the drug adsorption on plasma membrane and its intracellular uptake in living cells will be proposed through the disruption of the membrane fluidity.

Materials and methods

Cell lines. HCT-116 colon adenocarcinoma cell line was purchased from the ATCC (Manassas, VA, USA). The following cell types were routinely grown as monolayers in RPMI 1640 medium with Glutamax-1 (Gibco, UK) containing 10% fetal calf serum (Gibco, UK) at 37 °C in a humidified atmosphere of 5% CO_2 and underwent trypsinization (trypsin–EDTA (1×) in HBSS W/O CA&MG W/EDTA. 4NA, stored at −20 °C, Gibco, UK). The parental cell line was first cloned to obtain a reference SN38 sensitive clone, referred to as HCT-116 S. A continuous exposure of HCT-116 S to SN38 was carried out with stepwise increased concentrations ranging from 1 to 15 nM over a period of about 8 months. The cell population growing in 15 nM SN38 generated the HCT-116 R clone and overexpressed BCRP efflux proteins. A sulforhodamine test was determined after a 72 h treatment with mitoxantrone, and an IC_{50} of 2.8 and 11.1 nM was measured, respectively, for HCT-116 S and HCT-116 R.

Drug and chemicals. Mitoxantrone (MTX) and synthetic fluidizers benzyl alcohol (BA) and chloroform (CF) were purchased from Sigma (St. Louis, USA, $MW_{MTX} = 517.4$, $MW_{BA} = 108$, and $MW_{CF} = 119.38$). For SERS experiments, Ag sols were prepared as described by Lee and Meisel [15]. A 90 mg sample of $AgNO_3$ (ALFA, MW = 169.87) was suspended in 500 ml quartz-distilled water, purged with pure N_2, and heated to 100 °C. Ten milliliters of a 1% solution of sodium citrate (Sigma, USA, MW = 258.1), purged with N_2, was added dropwise to the boiling solution under vigorous stirring. The solution was kept boiling for 60–90 min. The absorption curve of the brownish suspension showed a maximum at 415 nm. One molar solutions of $NaClO_4$ (Sigma, St. Louis, USA, MW = 122.4), $MgSO_4$ (Sigma, St. Louis, USA, MW = 120), or NaCl (Prolabo, MW = 58.44) were used to aggregate Ag sols.

SERS spectroscopy. Micro-SERS experiments were performed with a Labram microspectrometer (Horiba Jobin Yvon), using a Titanium-Sapphire laser (Spectra Physics) tuned at 785 nm as excitation source. The microspectrometer is equipped with an Olympus model microscope and the measurements were recorded with a 100× objective (NA = 0.9) suitable for near infrared light. A 10^4 attenuating filter was inserted in the beam path to irradiate a single colloid aggregate by 20 μW. As dispersive element, the Labram microspectrometer is equipped with a holographic grating of 950 lines/mm giving a spectral resolution of 4 cm^{-1}. Micro-SERS spectra were recorded from 200 to 1800 cm^{-1}, with an acquisition time of 10 s. Macro-SERS spectra were obtained with an OMARS 89 spectrometer (DILOR, France). The diffraction was assured by a 1800 line/mm grating that allowed the analysis of a spectral window of about 400 cm^{-1} at a time. The detection system was constituted of 512 photodiodes coupled with a light amplifier. The excitation used for SERS experiments was the 514.6 nm line of an Ar^+ laser (Spectra Physics 2020-03 model). The theoretical spectral resolution was determined at 0.83 cm^{-1}. The spectrometer was linked to a computer, which allowed acquisition and mathematical processing of spectra with homemade software. The laser power was about 400 mW at samples. In these conditions, no contribution of Raman scattering from cells was observed.

A first series of tests determined aggregation conditions of silver colloid. Drug and cells were analyzed with isotonic Ag sols (diluted at V/V 30%, pH 7), aggregated by salts $NaClO_4$, or $MgSO_4$, or finally NaCl ($[salt]_{final} = 0.1$ M). NaCl salts allowed the highest Raman scattering. Different colloidal batches were tested with 10^{-8} M MTX and showed a reproducible drug Raman enhancement, validating a homogeneous colloidal preparation.

For micro-SERS experiments, cellular strains were treated with 2 μM MTX for 1 h at 37 °C in a humidified atmosphere of 5% CO_2 and washed twice with MTX-free RPMI medium (Gibco, UK). Each cell line was mixed with 500 μl isotonic aggregated colloid (pH 7). Colloid aggregates and cell culture were first visualized with a video camera. Stable aggregates, localized on cell surface, were irradiated one at a time with the laser beam. Each spectrum of MTX was obtained in focusing the laser line on one colloid grain in contact with the cell membrane. Presented spectra were representative of a series of five reproducible spectra of MTX-treated cells. In these conditions, no contribution of Raman scattering from untreated cells was observed. A control with 10^{-9} M MTX in solution was performed in focusing the laser line on a colloid grain in contact with the bottom of the petri dish.

For macro-SERS experiments, each cell type was treated with 2 μM MTX for 1 h at 37 °C in a humidified atmosphere of 5% CO_2, trypsinated, and washed twice with MTX-free RPMI medium (Gibco, UK) (3 min at 1000 rpm). Each population of cells was suspended in 50 μl isotonic aggregated colloid (pH 7) for SERS spectroscopy analysis. The viability of cells analyzed with silver hydrosol was checked by microscopy with 0.1% trypan blue test determining the cellular death percentage that was less than 0.5%. Each cell type was incubated in 1 mM BA or 1 mM CF for 10 min as described previously [16] to study the permeability influence of the plasma membrane on MTX adsorption preceding a treatment with 2 μM MTX for 1 h at 37 °C under a hydrated atmosphere with 5% CO_2. For each analysis series, a standard test with 10^{-8} M MTX validated the correct feature of the aggregated colloid. Each presented spectrum was a medium spectrum of 10^6 MTX-treated cells resulting from 20 accumulations of 3 s each and was representative of a series of three reproducible spectra of three different cell batches. For different graphs (Fig. 2), each reported measurement corresponded to the band area (1250 and 1350 cm^{-1}) of SERS average spectrum. Significance of results was determined by Student's t test. The level of significance chosen was 99% ($P < 0.01$).

Confocal fluorescence microscopy. Fluorescence microscopy was performed using an MRC-1024 confocal system (Bio-Rad, Microscience, Hemel Hempsted, UK). The scanning confocal system was

coupled with an Optiphot epifluorescence microscope (Nikon, Tokyo, Japan), equipped with a 60× magnification water immersion objective of numerical aperture NA = 1.4. Experiments were performed with a Kr^+/Ar^+ laser at 568 nm. MTX emission was collected through a 680 nm band-pass filter. Cell types were treated with 5 μM MTX, with or without an incubation with 10 mM BA or 10 mM CF for 1 h at 37 °C in a humidified atmosphere of 5% CO_2, and washed in MTX-free RPMI medium to locate drug fluorescence emission. Images were recorded with LaserSharp Version 2.1 T (Bio-Rad software) and were calculated with Confocal Assistant (Bio-Rad software). Each image was represented with 512×512 pixels of 0.1×0.1 μm each, and acquired with a Kalman filter to reduce background noise (average on 3 scanning images).

Spectrophotometric measurements of MTX accumulation. Intracellular MTX accumulation was quantified in both cell types by spectrophotometric measurements using UVIKON Spectrophotometer (Kontron Instruments, Italy). Five hundred microliters of a cellular lysate was analyzed between 550 and 680 nm with a 50 nm/min speed scanning. A reference range of MTX in solution was carried out between 10^{-7} and 10^{-5} M concentrations to validate this method. After a linear baseline subtraction, the intracellular uptake of MTX was estimated from the value of drug absorbance spectra at the maximum 622 nm, referred to as a reference range and reported in 10^6 cells. Treated cells were lysed in 1% Triton X-100 (Sigma, USA) for 5 min at room temperature before absorbance reading.

Results

Confocal microscopy imaging of MTX

HCT-116 S and R were treated with MTX to observe the cellular layout. The two cell strains were treated with 5 μM MTX for 1 h at 37 °C in a hydrated atmosphere with 5% CO_2. After washing in MTX-free RPMI at 4 °C, cells were observed by confocal microscopy (Fig. 1). Image of MTX-treated HCT-116 S displayed a high fluorescence emission in cytoplasm and nucleoli. In contrast, the MTX fluorescence distribution in HCT-116 R mainly located around the plasma membrane in spite of several plotted organelles.

MTX-treated HCT-116 S and R were incubated with 10 mM benzyl alcohol (BA) or chloroform (CF) in the same conditions to observe the effect of fluidizers on MTX intracellular layout. For HCT-116 S, a slight increase of MTX emission was observed. Compared to their control MTX-treated HCT-116 R incubated with BA or CF revealed clearly a higher MTX fluorescence emission in nuclei and cytoplasm. In addition, BA and CF slightly decreased the MTX fluorescence emission next to the plasma membrane.

Modulation of MTX influx

A quantification of the intracellular MTX was performed in both cell types to determine the influence of fluidizers on the MTX influx. HCT-116 S and R were treated with 5 μM MTX with or without 10 mM BA or CF for 1 h at 37 °C in a hydrated atmosphere with 5% CO_2 preceding an optical density analysis at 622 nm (Fig. 2, graph 1). At 37 °C, the intracellular accumulation of MTX in HCT-116 S showed a 2.5-fold higher MTX accumulation (about 447 ± 67 pmol/10^6 cells) in comparison with that in HCT-116 R (about 191 ± 28 pmol/10^6 cells). An incubation of MTX-treated HCT-116 S with BA or CF revealed a 1.9- and

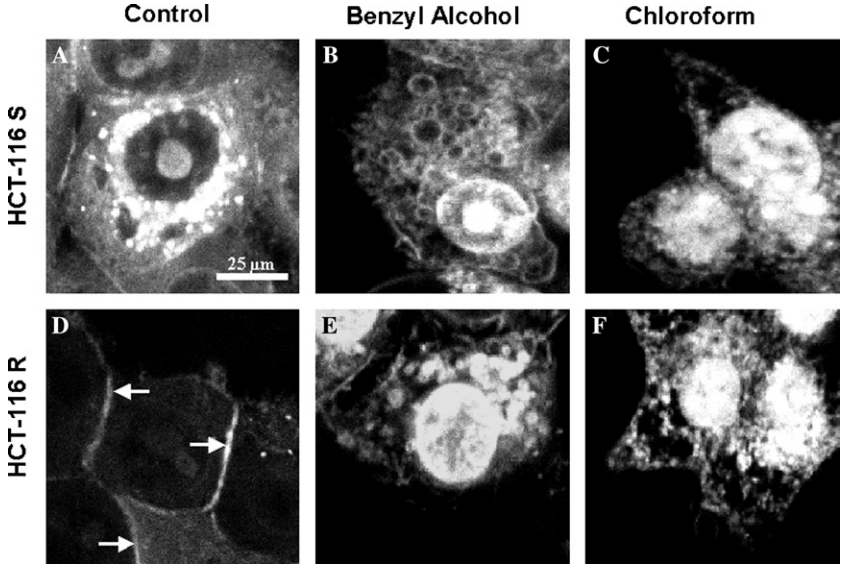

Fig. 1. Confocal fluorescence microscopy images of MTX emission in sensitive HCT-116 S (A–C) and resistant HCT-116 R (D–F) cells. Each cell type was incubated with MTX (A,D) and fluidizers benzyl alcohol (B,E) or chloroform (C,F). An exclusive MTX emission around plasma membrane of resistant cells (white arrows) is observed whereas fluidizers increase the intracellular uptake of MTX in both cell lines at the same time with a less MTX emission around the plasma membrane. Experimental conditions: each cell type was treated with 5 μM MTX for 1 h at 37 °C and incubated with 10 mM benzyl alcohol or chloroform; laser excitation was fixed at 568 nm and MTX emission was collected through a 680 nm band-pass filter. Each image corresponds to 512×512 pixels, each of 0.1×0.1 μm^2 size.

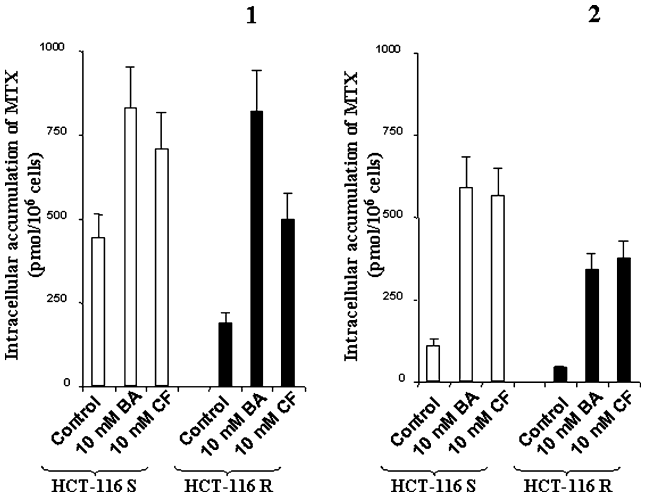

Fig. 2. Improved effects of fluidizers benzyl alcohol or chloroform on MTX influx in sensitive (HCT-116 S) and resistant (HCT-116 R) cells at 37 °C (graph 1) or 4 °C (graph 2). Experimental conditions: each cell type was treated with 5 μM MTX with or without 10 mM benzyl alcohol or chloroform for 1 h either at 37 °C or at 4 °C to block BCRP activity and to decrease the natural fluidity of plasma membrane. Each value was obtained by absorbance reading at 622 nm; the intracellular concentration of MTX was calculated from a range standard and reported in pmol/10^6cells. Results are mean values of three experiments ± SD. $P < 0.01$.

1.6-fold higher drug accumulation, respectively. MTX-treated HCT-116 R incubated with BA or CF showed a 4.3- and 2.6-fold increase of the intracellular MTX accumulation, respectively.

An incubation of both cell lines with 5 μM MTX for 1 h was carried out at 4 °C to inhibit efflux pump BCRP and to rigidify phospholipidic bilayer (Fig. 2, graph 2). At 4 °C the same 2.5-fold factor of intracellular MTX accumulation was observed between resistant (42 ± 6 pmol/10^6 cells) and sensitive (115 ± 17 pmol/10^6 cells) cells compared at 37 °C. Thus, this result allowed us to conclude that the difference of MTX intracellular accumulation between these two cell strains was not exclusively dependent on efflux protein overexpression. Moreover, a 5.2- and 4.9-fold increase of MTX accumulation in HCT-116 S incubated with BA or CF was observed, respectively. At the same time, an 8.1- and 9-fold higher MTX accumulation in HCT-116 R incubated with BA or CF, respectively. The increase factor of MTX accumulation was higher with fluidizers for resistant cells than for its sensitive strain. Fluidizers antagonize rigidified effect of temperature on membrane behavior at 4 °C. Results confirmed observations of increased fluorescence emission of intracellular MTX by confocal microscopy.

Modulation of MTX adsorption for the plasma membrane

The SERS method was applied to characterize an adsorption of MTX on a cellular membrane. A specific drug interaction with the plasma membrane could be demonstrated by differences of SERS spectra compared to MTX in solution. Each spectrum of MTX was obtained by micro-SERS analysis in focusing the laser line on one colloid grain in contact with the membrane of treated cells. HCT-116 S were incubated in 2 μM MTX for 1 h at 37 °C, washed twice in drug-free RPMI, and mixed with isotonic pre-aggregated colloid before micro-SERS analysis (Fig. 3). Modifications of the 475 and 517 cm^{-1} bands were observed for membrane-adsorbed MTX spectra (full line in Fig. 3A) compared to drug in solution (dot line in Fig. 3A). Moreover, a significant shift of the 1307 cm^{-1} band toward 1303 cm^{-1} was determined for MTX adsorbed with cells (Fig. 3B). The drug spectral fingerprint allowed us to discrim-

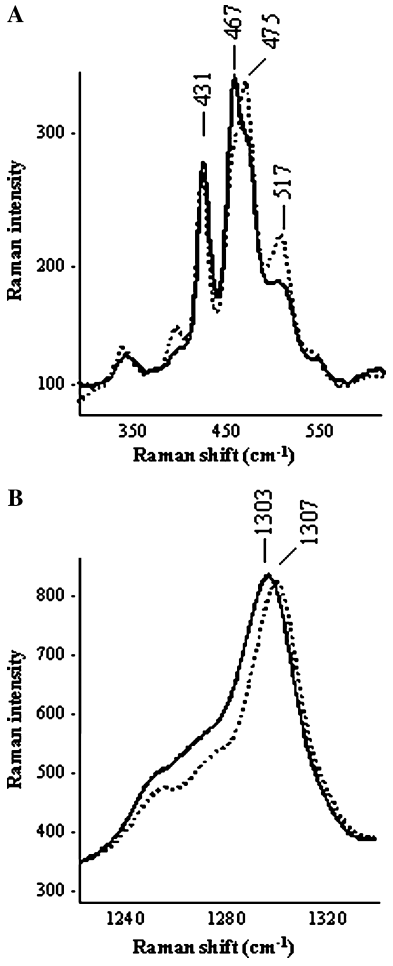

Fig. 3. Discrimination of MTX adsorbed on the plasma membrane of sensitive cells from drug in solution by micro-SERS spectroscopy. SERS spectra of MTX adsorbed on membrane (in full line) and MTX in solution (in dot line) between 300 and 600 cm^{-1} (A), and between 1220 and 1340 cm^{-1} (B). Spectra were normalized on the 431 cm^{-1} band (A) and on the 1177 cm^{-1} band (B). Experimental conditions: laser line was focused on one colloid grain in contact with cellular membrane or at the bottom of the petri dish for MTX in solution; for each spectrum: 20 μW laser power (785 nm of titanium-sapphire line) at sample and 1 accumulation of 10 s.

inate clearly MTX adsorption phenomena on plasma membrane from drug in solution.

Spectral profiles were reproducible whereas a high intensity variability was noticed on whole SERS spectra depending on each nanoparticle size. Thus, next experiments were carried out by macro-SERS spectroscopy on 10^6 cells in a 50 μl colloid volume, to avoid this variability. In this aim, HCT-116 S and R were incubated in increased MTX concentrations ranging from 0.1 to 2 μM for 1 h at 37 °C, trypsinated, and washed twice in MTX-free RPMI at 4 °C. About 10^6 cells were mixed with isotonic pre-aggregated colloid (Fig. 4). A 3-fold higher intensity was observed for MTX-treated HCT-116 R compared to HCT-116 S at each drug concentration. This result involved a tight MTX adsorption in the plasma membrane microenvironment. The variation coefficient (VC) of MTX Raman enhancement was calculated from the 1250 to 1350 cm^{-1} area band on three different cell batches and was estimated to be about 29% for MTX-treated sensitive cells and 17% for resistant cells, concluding that the difference of MTX Raman diffusion between resistant and sensitive cells was significant ($P < 0.01$). Moreover, tests with other colloidal batches demonstrated a reproducible VC between both cell lines.

BA or CF was added to cells during treatment with MTX to determine the changes in consequences of membrane structure on MTX adsorption. Each cell type was incubated in increased MTX concentrations (0.1–2 μM) with 1 mM BA or CF at each time for 1 h at 37 °C (Fig. 4). A 3-fold decrease of MTX Raman intensity was observed for MTX-treated HCT-116 R incubated with BA or CF whereas no intensity change for HCT-116 S incubated with BA or CF was observed (see insert in Fig. 4). The difference of MTX Raman diffusion for resistant cells incubated with or without fluidizers was significant ($P < 0.01$). Addition of BA and CF agents resulted in modulating MTX adsorption on the plasma membrane of HCT-116 R, exclusively.

The MTX release from the membrane microenvironment was carried out at 4 °C to reveal differences between drug affinity and the membrane bilayer in the absence of BCRP ATPase activity. Each cell type was treated with 2 μM MTX with or without 1 mM BA or CF for 1 h at 37 °C. Then, cells were washed (time $T = 0$) and added to fluidizer- and MTX-free RPMI at 4 °C before SERS analysis (Fig. 5). A rapid decrease of MTX SERS intensity was observed for MTX-treated HCT-116 R from 10 min in MTX-free RPMI whereas no spectral change for MTX-treated HCT-116 S occurred. The observed decrease of SERS diffusion in resistant cells corresponded to a MTX release out of a membrane microenvironment. The higher MTX scattering on HCT-116 R, followed by a rapid drug release from plasma membrane in medium, could reveal a specific adsorption site of MTX. Moreover, a little change of SERS intensities occurred in the presence of fluidizers during the MTX release from the plasma membrane at 4 °C. The fluidizer, either BA or CF, should disrupt this specific site exclusively.

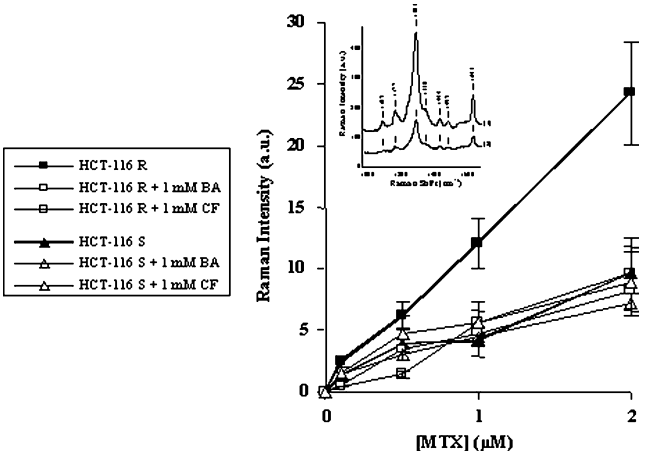

Fig. 4. Influence of the MTX concentration (0.1–2 μM MTX for 1 h at 37 °C) on drug adsorption on resistant (HCT-116 R) and sensitive (HCT-116 S) cell membrane pre-incubated with or without 1 mM membrane fluidizers benzyl alcohol or chloroform by SERS spectroscopy. Each reported value (a.u.) corresponds to the integrated intensity of SERS spectra between 1250 and 1350 cm^{-1}. Experimental conditions: about 10^6 cells were used, for each spectrum: 400 mW laser power (514 nm of Ar^+ line) at sample and 20 accumulations of 3 s. each. Results are mean values of three experiments ± SD. $P < 0.01$. Inset in figure: an average SERS spectrum of 10^6 resistant (1) or sensitive (2) cells treated with 1 μM MTX 1 h at 37 °C.

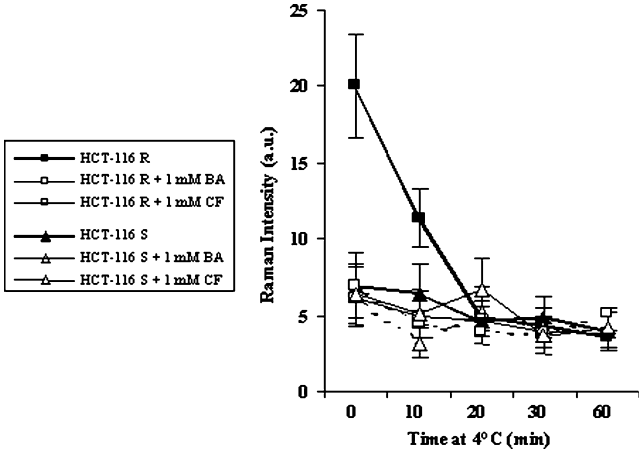

Fig. 5. Release of adsorbed MTX at 4 °C from the plasma membrane of HCT-116 R and S pre-incubated with or without membrane fluidizers benzyl alcohol or chloroform. Cells were incubated in 2 μM MTX with or without 1 mM benzyl alcohol or chloroform for 1 h at 37 °C and at time 0, cells were added to MTX- and fluidizer-free medium for different time laps (0–60 min). Each reported value (a.u.) corresponds to the integrated intensity of SERS spectra between 1250 and 1350 cm^{-1}. Experimental conditions: about 10^6 cells were used, for each spectrum: 400 mW laser power (514 nm of Ar^+ line) at sample and 20 accumulations of 3 s. each. Results are mean values of three experiments ± SD. $P < 0.01$.

Discussion

The interaction of anticancer drugs like doxorubicin or MTX with membranes has been intensively studied with the use of various methods including spectroscopic techniques [11,12,17,18]. The details of drug interactions with plasma membrane are crucial in the understanding of their diffusion kinetics. Membrane lipid changes between sensitive and resistant cells have been described to be associated with MDR phenotype [3,19]. Plasma membrane lipid bilayer reveals a dozen of different lipid species whose distribution is far from homogeneous due to the presence of microdomains such as lipid raft and caveolae [20]. Several studies of fluorescence with TMA-DPH probe have revealed a reduced fluidity of membrane for resistant cells compared to parental lines [3,8]. The intracellular accumulation decrease of a cytotoxic compound could be due to a slower drug diffusion across the membrane, depending on the nature of phospholipidic entities and the bilayer structure [1]. Specific affinities of MTX with membrane components are not well known. Besides, using electron spin resonance (ESR) and fluorescence spectroscopy, Marczak et al. [18] have shown that MTX led to a disturbance in the structure of membrane lipids and proteins on erythrocytes. Thus, MTX may interact with phospholipids or with the negative charged lipids.

We previously reported that an increase of SERS intensity could be attributed to an additional adsorption site for resistant cells, since the difference of 3-fold SERS intensity between MTX-treated HCT-116 R and S rapidly disappeared in a MTX-free medium at 4 °C [12]. These results could correspond to a quick release of MTX from an unstable adsorption site on the plasma membrane of resistant cells, exclusively. This study related the consequences of this additional adsorption site for HCT-116 R to the lower drug uptake. In a medium at 4 °C to inhibit BCRP efflux pump, a cellular incubation in MTX also showed a 2.5-fold lower accumulation of drug in HCT-116 R compared to its sensitive line. Drug permeability differences between resistant and sensitive cells should occur in spite of an efflux mechanism. The source of this permeability difference between both cell lines remains to be defined. Addition of BA or CF produced a high decrease of the MTX SERS intensity for HCT-116 R. The increase of the membrane fluidity affected only the supplementary adsorption site of MTX on resistant cells. In addition, the lower intracellular uptake of MTX in HCT-116 R was widely dependent on cohesion of the plasma membrane, since BA and CF disrupted membrane fluidity speeded up MTX flip-flop. Influx experiments showed that fluidizers increase largely the intracellular accumulation of MTX in both cell lines, irrespective of the temperature of medium. Besides, we have already observed BA or CF inhibit the MTX efflux on HCT-116 R (data not shown). Regev et al. [13] have described modulating effects of different membrane fluidizers on Pgp ATPase activity and on the intracellular concentration of doxorubicin. BA and CF should change deeply the membrane structure and drug adsorption of resistant cells. These changes could favor the intracellular accumulation of MTX both by increasing the drug uptake and inhibiting the BCRP efflux pump.

In conclusion, SERS spectroscopy appears as an informative method for the study of drug binding to the plasma membrane of living cells. We have revealed that resistant cells should present a higher drug adsorption in their plasma membrane concluding to a supplementary binding site of drug. The higher adsorption on resistant cells could correspond to a change of membrane structure, since membrane permeation disrupts MTX adsorption on plasma membrane and increases intracellular uptake of MTX.

References

[1] R.J. Veldman, S. Zerp, W.J. van Blitterswijk, M. Verheij, N-hexanoyl-sphingomyelin potentiates in vitro doxorubicin cytotoxicity by enhancing its cellular influx, Br. J. Cancer 90 (2004) 917–925.
[2] G.D. Leonard, T. Fojo, S.E. Bates, The role of ABC transporters in clinical practice, Oncologist 8 (2003) 411–424.
[3] A.B. Hendrich, K. Michalak, Lipids as a target for drugs modulating multidrug resistance of cancer cells, Curr. Drug Targets 4 (2003) 23–30.
[4] V.Y. Erukova, O.O. Krylova, Y.N. Antonenko, N.S. Melik-Nubarov, Effect of ethylene oxide and propylene oxide block copolymers on the permeability of bilayer lipid membranes to small solutes including doxorubicin, Biochim. Biophys. Acta 1468 (2000) 73–86.
[5] M. Przybylska, Z. Jozwiak, Relevance of drug uptake, cellular distribution and cell membrane fluidity to the enhanced sensitivity of Down's syndrome fibroblasts to anticancer antibiotic-mitoxantrone, Biochim. Biophys. Acta 1611 (2003) 161–170.
[6] M.F. Lecompte, G. Laurent, J.P. Jaffrezou, Sphingomyelin content conditions insertion of daunorubicin within phosphatidylcholine monolayers, FEBS Lett. 525 (2002) 141–144.
[7] R. Regev, G.D. Eytan, Flip-flop of doxorubicin across erythrocyte and lipid membranes, Biochem. Pharmacol. 54 (1997) 1151–1158.
[8] M. Jedrzejczak, A. Koceva-Chyla, K. Gwozdzinski, Z. Jozwiak, Changes in plasma membrane fluidity of immortal rodent cells induced by anticancer drugs doxorubicin, aclarubicin and mitoxantrone, Cell Biol. Int. 23 (1999) 497–506.
[9] H. Schuldes, J.H. Dolderer, G. Zimmer, J. Knobloch, R. Bickeboller, D. Jonas, B.G. Woodcock, Reversal of multidrug resistance and increase in plasma membrane fluidity in CHO cells with R-verapamil and bile salts, Eur. J. Cancer 37 (2001) 660–667.
[10] P.R. Wielinga, H.V. Westerhoff, J. Lankelma, The relative importance of passive and P-glycoprotein mediated anthracycline efflux from multidrug-resistant cells, Eur. J. Biochem. 267 (2000) 649–657.
[11] C. Heywang, M. Saint-Pierre Chazalet, C.M. Masson, J. Bolard, Orientation of anthracyclines in lipid monolayers and planar asymmetrical bilayers: A surface-enhanced resonance Raman scattering study, Biophys. J. 75 (1998) 2368–2381.

[12] G. Breuzard, J.F. Angiboust, P. Jeannesson, M. Manfait, J.M. Millot, Surface-enhanced Raman scattering reveals adsorption of mitoxantrone on plasma membrane of living cells, Biochem. Biophys. Res. Commun. 320 (2004) 615–621.
[13] R. Regev, Y.G. Assaraf, G.D. Eytan, Membrane fluidization by ether, other anaesthetics, and certain agents abolishes P-glycoprotein ATPase activity and modulates efflux from multidrug-resistant cells, Eur. J. Biochem. 259 (1999) 18–24.
[14] I. Nabiev, G.D. Chumanov, R.G. Efremov, Surface-enhanced Raman scattering spectroscopy of biomolecules. Part II. Application of short- and long-range components of SERS to study of the structure and function of membrane proteins, J. Raman Spectrosc. 21 (1990) 49–54.
[15] P.C. Lee, D. Meisel, Adsorption and surface-enhanced Raman of dyes on silver and gold sols, J. Phys. Chem. 86 (1982) 3391–3395.
[16] P.J. Butler, G. Norwich, S. Weinbaum, S. Chien, Shear stress induces a time- and position-dependent increase in endothelial cell membrane fluidity, Am. J. Physiol. Cell Physiol. 280 (2001) C962–969.
[17] L. Gallois, M. Fiallo, A. Garnier-Suillerot, Comparison of the interaction of doxorubicin, daunorubicin, idarubicin and idarubicinol with large unilamellar vesicles. Circular dichroism study, Biochim. Biophys. Acta 1370 (1998) 31–40.
[18] A. Marczak, A. Wrzesien-Kus, E. Krykowski, T. Robak, Z. Juzwiak, The interaction of daunorubicin and mitoxantrone with the red blood cells of acute myeloid leukemia patients, Cell. Mol. Biol. Lett. 8 (2003) 885–890.
[19] J.H. Dolderer, G. Zimmer, B.G. Woodcock, H. Bockhorn, R. Bickeboller, H. Schuldes, Resistance modulation in CHO cells by R-verapamil and bile salts is associated with physical and chemical changes in the cell membrane, Int. J. Clin. Pharmacol. Ther. 38 (2000) 196–203.
[20] Y. Lavie, M. Liscovitch, Changes in lipid and protein constituents of rafts and caveolae in multidrug resistant cancer cells and their functional consequences, Glycoconj. J. 17 (2000) 253–259.